



HPU2 Journal of Sciences: Natural Sciences and Technology

journal homepage: <https://sj.hpu2.edu.vn>



Article type: Research article

The roles of intermediate fluorophores on the optical properties of bottom-up synthesized carbon nanodots

Duy-Khanh Nguyen^{a,*}, Quang-Trung Le^b, Xuan-Dung Mai^c, Thanh-Son Le^a

^aDepartment of Chemistry, Hanoi National University, 334 Nguyen Trai, Hanoi.

^bDepartment of Chemistry, Chonnam National University, 500-757 Gwangju, Republic of Korea

^cDepartment of Chemistry Hanoi Pedagogical University 2, 32 Nguyen Van Linh, Phuc Yen, Vinh Phuc, Vietnam

Abstract

Carbon nanodots (CNDs) are the latest nano-sized carbon materials having unique properties such as biocompatible, highly photoluminescent, and nontoxic which are suitable for diverse applications including lighting, sensing, bioimaging, and biochemical analyzing. CNDs could be synthesized by top-down methods in which graphite is fragmented into nano-sized graphene dots. Alternatively, CNDs could be formed by a bottom-up synthetic strategy where organic molecules are fused together via complex condensation and carbonization processes. Although a great number of organic molecules have been used successfully to prepare CNDs there are very few CNDs that exhibit the quantum size effects. The absorption and emission properties of bottom-up synthesized CNDs rely vastly on molecular-like fluorophores which are the intermediates formed during the fusion of molecular precursors and are incorporated into CNDs in the later states of carbonization processes. This review aims to demonstrate recent understandings on the formation of intermediate fluorophores and their contribution to the optical properties of CNDs.

Keywords: Carbon nanodots, Carbon quantum dots, Bottom-up, Fluorophore, Mechanism.

1. Introduction

Inorganic quantum dots (QDs) such as CdX and PbX (X=S, Se, Te) provide fine-tunable nano-sized building units for the construction of diverse nanoarchitectures for a wide range of applications including (but not limited to) solution-processed optoelectronics, fluorescence-based sensors, and

* Corresponding author, E-mail: ndkhanh4o@gmail.com

<https://doi.org/10.56764/hpu2.jos.2023.2.2.68-82>

Received date: 20-8-2023 ; Revised date: 31-8-2023 ; Accepted date: 31-8-2023

This is licensed under the CC BY-NC-ND 4.0

fluorescence-based probes. However, the inherent toxicity related to heavy metals inhibits their practical applications, especially in bio-related fields [1]. Therefore, the development of biocompatible QDs have been strongly demanded to replace Cd-based QDs in various biological and medical applications. Since the first report in 2004 [2] water-soluble and fluorescent carbon nanodots (CNDs) have attracted increasing researches that have now described CNDs to be low-toxicity [3], tunable emission color in the visible and near infrared regions [4], low cost [5], [6], and applicable to diverse fields including light-emitting diodes (LEDs), photocatalyst, bioimaging, and sensing. Nevertheless, the chemical structure and luminescent mechanism of CNDs are still not fully understood. In this review, we will address the recent understandings on the structure of CNDs as well as the contribution of molecular-like fluorophores to the optical properties of CNDs. We indeed hope that this review can provide understandings on the relation between the chemical structure and the optical properties of CNDs, especially bottom-up synthesized CNDs that could help ones to design CNDs for target applications.

2. The evolution of the structure of bottom-up synthesized carbon nanodots

Carbon nanodots (CNDs) or carbon quantum dots (CQDs) were first observed by X. Xu and coworkers as fluorescent nanoparticles when they purified carbon nanotube from arc-discharge soot [2]. The fact that the aqueous solutions of nanoparticles exhibit intense luminescence in the visible region has attracted increasing scientists to explore CNDs in diverse aspects with the hope to replace Cd-based quantum dots in many applications where the toxicity of materials is concerned. CNDs became a new member of zero-dimensional carbon nanomaterials as shown in Fig. 1 [7]. The structure of a CND was modeled as an assembly of polycyclic aromatic hydrocarbons (PAHs) attracting together via π - π interactions or being embedded in a carbogenic matrix, Fig. 2a [8]. PAHs alone surely follow the quantum confinement effects, i.e. the energy gap decreases as the size of PAH increases. Therefore, when CNDs compose of a few layers of PAHs, which are usually named as graphene quantum dots, the CNDs will exhibit the quantum size effects, e.g. the emission color red-shifts as the diameter of CNDs increases, Fig. 2b [9], [10]. Shuit-Tong Lee group used an electrochemical oxidation method to cut graphite rod into CNDs having a diameter ranging from 1.2 to 3.8 nm and demonstrated size-dependent fluorescence [11]. Recently, F. Yuan and co-workers demonstrated that triangular CNDs prepared by hydrothermal treatment of phloroglucinol exhibited narrow emission spectra and quantum size effects [12].

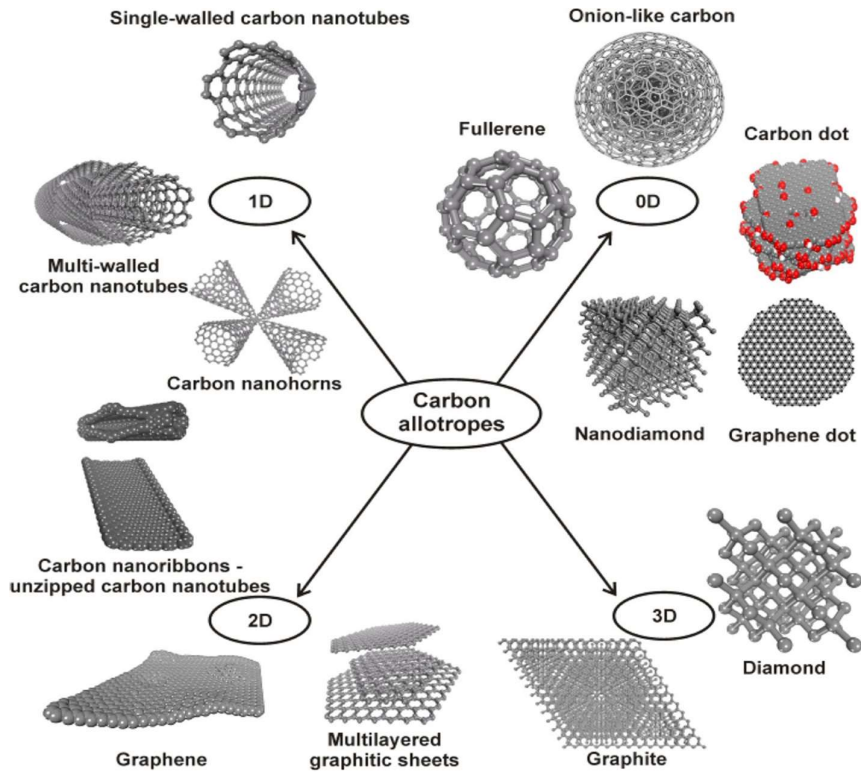


Figure 1: The classification of carbon nanomaterials according to the dimensionality. Carbon nanodots is a new member of 0D dimensional carbon nanomaterials in which the charges are confined in all three dimensions [7].

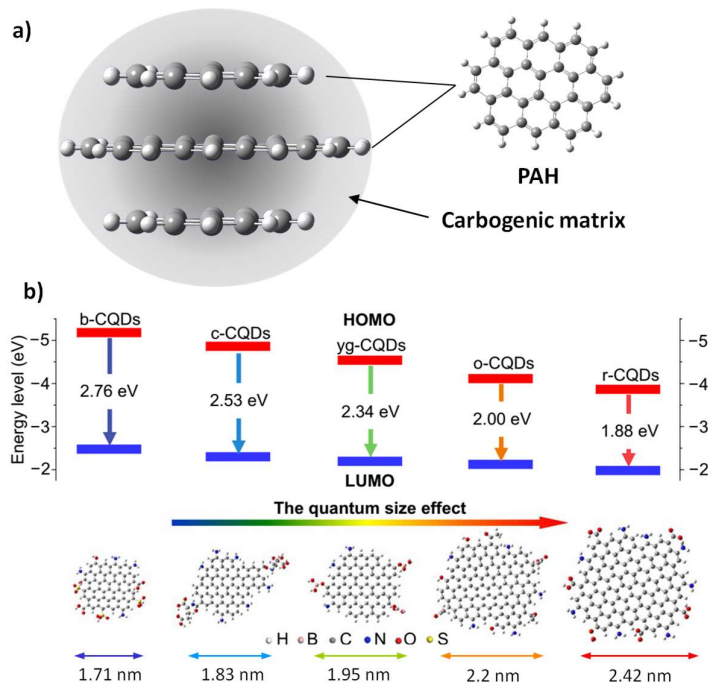


Figure 2: a) Schematic structure of a carbon nanodot; b) The size-dependent energy levels of graphitic carbon nanodots [9].

In the cases of inorganic quantum dots such as CdX and PbX (X=S, Se, Te) the capping ligand could be exchanged from one to another to tune the solubility while almost maintaining the band gap of the dots. One of striking characters of CNDs is that their electronic structure is strongly influenced by the surficial functional groups, especially in the cases that CNDs have one graphitic layer [13]. S. Jeon observed that the bandgap of CNDs synthesized from graphene oxide decreased with increasing the number of amino functional groups [14]. The effects of the functional groups could be understood from DFT calculations based on naphthalene model shown in Fig. 3. Both $-CHO$ and $-NH_2$ change significantly the HOMO and LUMO energy levels because the conjugation system which is regarded as the confinement space of PAH extends to the functional groups. Because of the covalence bonds between PAH and surficial groups the confinement space needs to be treated not only PAH but also the surface groups. The absorption and emission of CNDs that involve orbitals influenced by surficial groups such as HOMO and LUMO shown in Fig. 3 are affected by solvation medium due to the local interactions between solvent molecules and the functional groups, Fig. 4 [15], [16].

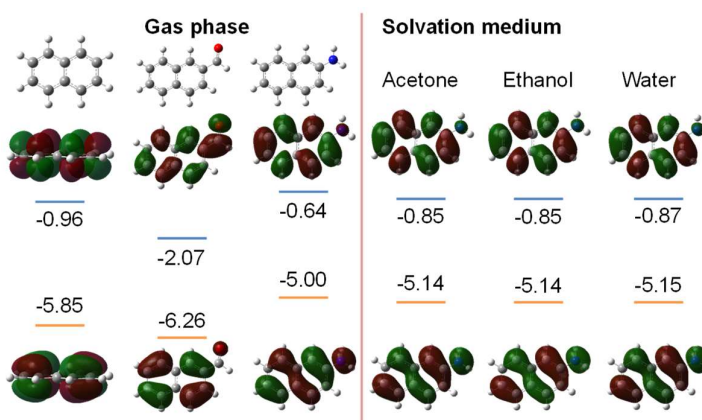


Figure 3: Effects of functional groups and solvation medium on the energy levels. DFT calculations were conducted on naphthalene model using B3LYP function using 6.31g basic set. $-CHO$ and $-NH_2$ were used as functional groups.

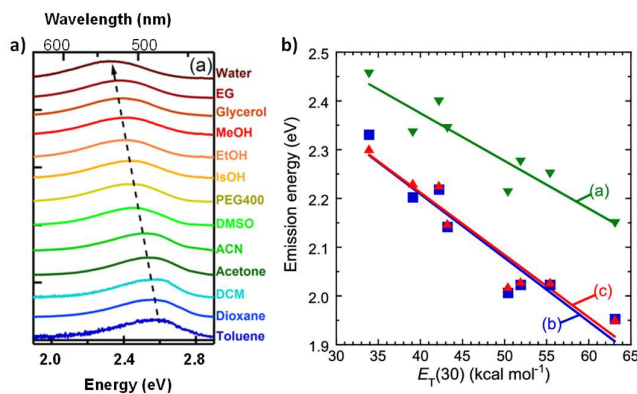


Figure 4: a) Normalized emission spectra of CNDs dissolved in different solvents. Adapted with permission from ref [15], Copyright 2016, American Chemical Society. b) Effects of solvent polarity parameter ($E_T(30)$) on the emission energy of CNDs synthesized from (a): *o*-phenylenediamine, (b): *m*-phenylenediamine, and (c): *p*-phenylenediamine [16].

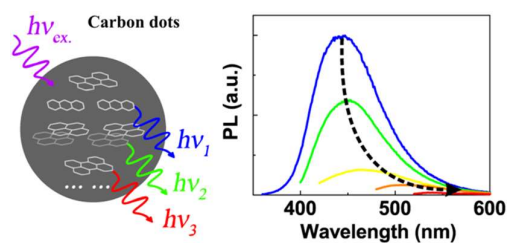


Figure 5: The excitation dependence of photoluminescence of CNDs is attributed to the energy transferring among PAHs within CNDs. Adapted with permission from ref [8], Copyright 2015, American Chemical Society.

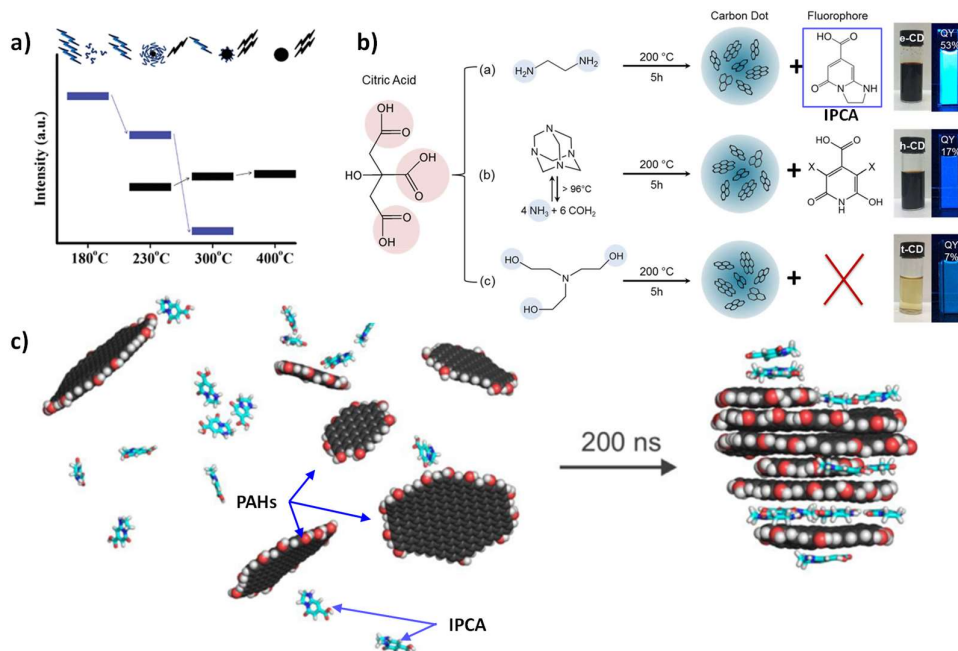


Figure 6: **a)** The contribution of molecular fluorophore (blue) and carbogenic core (black) to the emission of CNDs obtained at different pyrolysis temperature. Adapted with permission from ref [17], Copyright 2012, American Chemical Society. **b)** IPCA fluorophore accounts for the high photoluminescence of CNDs synthesized from citric acid and amines. Adapted with permission from ref [18], Copyright 2016, American Chemical Society. **c)** Molecular dynamics shows the self-assembling of IPCA and PAHs into quasi-spherical CNDs in an aqueous medium. Reprinted with permission from ref [19]. Copyright 2021 Elsevier.

In addition to contribution of surficial groups to the optical properties of CNDs the interactions among PAHs within CNDs that could even lead to ultimate orbital hybridizations [20] make the electronic transitions within a CND be more complicated. M. Fu and coworkers demonstrated that a physical mixture of anthracene, pyrene, and perylene exhibited excitation-dependent photoluminescence that was similar to CNDs synthesized from citric acid (CA) and ethylenediamine (EDA) [8]. The authors explained the excitation dependence of CNDs to be due to the fact that subsets of PAHs can be excited at different wavelength and the resultant excitons migrate to the larger PAHs, Fig. 5.

In parallel to top-down synthetic strategy, there have been number of methods to prepare CNDs using molecular precursors which could be either pure chemicals or components extracted from

natural resources. The bottom-up synthetic strategy uses heat to induce series of condensation and carbonization reactions that fuse precursors into CNDs. M. J. Krysmann [17] found the existence of an amide fluorophore that is formed by pyrolysis CA and EDA at 180°C. The fluorophore contributes to the emission of CNDs in addition to a carbogenic core and its contribution decreases as the pyrolysis temperature increases, Fig. 6a. The fluorophore was recognized to be 5-oxo-1,2,3,5-tetrahydroimidazo[1,2- α]pyridine-7- carboxylic acid (IPCA) [21] which is an intermediate formed via condensation between CA and EDA. IPCA dominates the optical properties of CNDs, Fig. 6b [18], [22]. The formation of IPCA can occur in aqueous medium, poly(vinylalcohol) [23], Poly(methyl methacrylate) [24], and even on the surfaces of carboxyl-terminated CNDs [25]. By using theoretical calculations, M. Otyepka group showed that IPCA molecules assembly via π - π interactions to form seeds of CNDs and they also stack with PAHs forming CNDs [19], [26]. The structure was also confirmed by NMR spectroscopy [27].

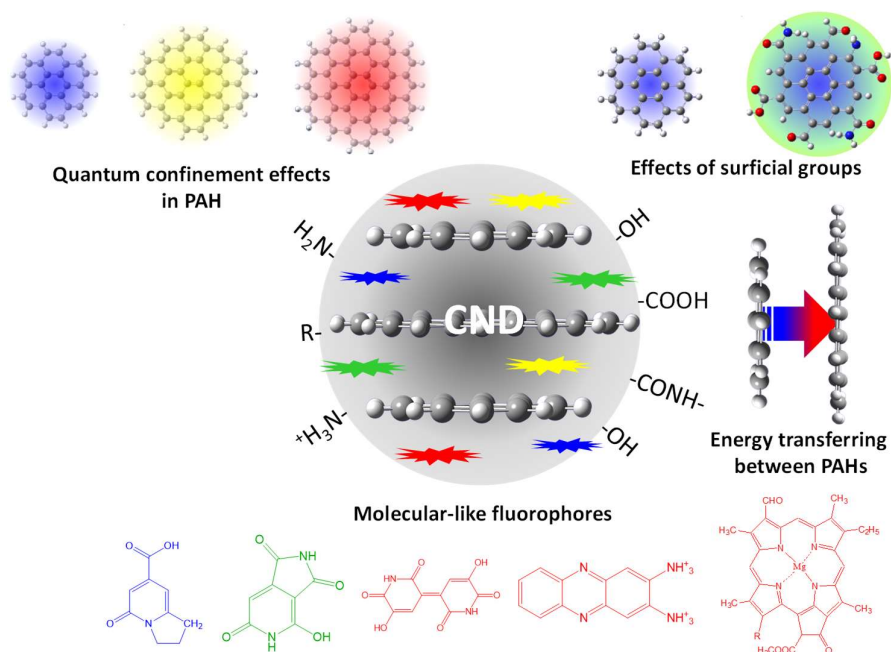


Figure 7: A model of CNDs containing PHAs and molecular fluorophores embedded in a carbogenic core. The quantum confinement effects, surficial functional groups, interactions between PAHs, and type of fluorophores influence the optical properties of CNDs.

To sum up, there are more than one factors that influence the optical properties of CNDs depending on the complexity of the CND structure as illustrated in Fig. 7. A bottom-up synthesized CND usually contains surface simple groups, PHAs, molecular-like fluorophore, and carbogenic matrix. The surface simple groups such as $-\text{COOH}$, $-\text{NH}_2$, $-\text{OH}$, or alkyl determine the solubility of CNDs in different solvents and the reactivity of CNDs to other reagents when ones regard CNDs as a starting material to construct multiple functional materials. PAHs themselves exhibit quantum size effects that could extend to the surficial groups. Additionally, PAHs tend to assembly via π - π interactions that enhance the energy transferring from the smaller PAHs to the bigger PHAs [28], [29] and account for the red-shifting of the emission spectrum upon increasing the excitation wavelength. Molecular – like fluorophores act as an emitting center in CNDs and in many cases, they determine the emission color of CNDs. We will summary some important fluorophores that have been reported so far.

3. Blue-emitting fluorophores

3.1. Citrazinic acid

Andrey L. Rogach group prepared CNDs from citric acid (CA) and ammonia using a solvothermal method in either aqueous or supercritical ammonia conditions and demonstrated that the absorption and emission properties of CNDs arise from citrazinic acid fluorophore [30]. The results were further improved by theoretical calculations [31]. The CNDs exhibit a distinct absorption band at 341 nm corresponding to π - π^* transition in citrazinic acid fluorophore whose formation was proposed in Fig. 8b.

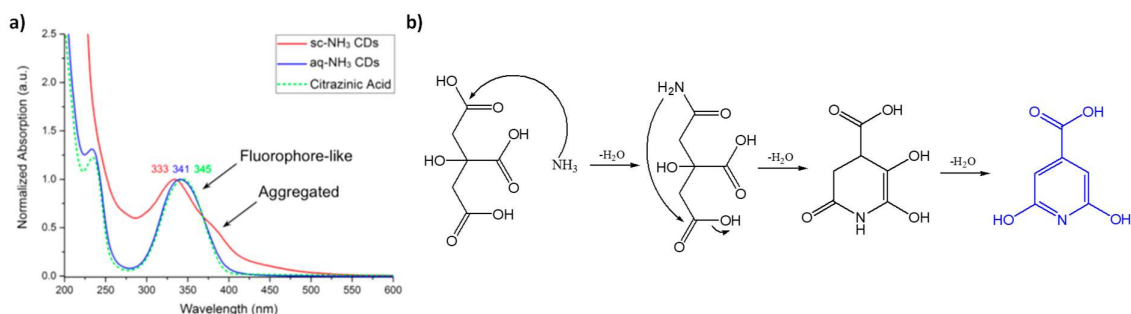


Figure 8: a) The absorption spectra of CNDs prepared from citric acid and ammonia in aqueous (aq-NH₃ CNDs) and supercritical ammonia (sc-NH₃ CNDs) in comparison with the absorption profile of citrazinic acid. b) The formation mechanism of citrazinic acid [30].

3.2. IPCA and derivatives

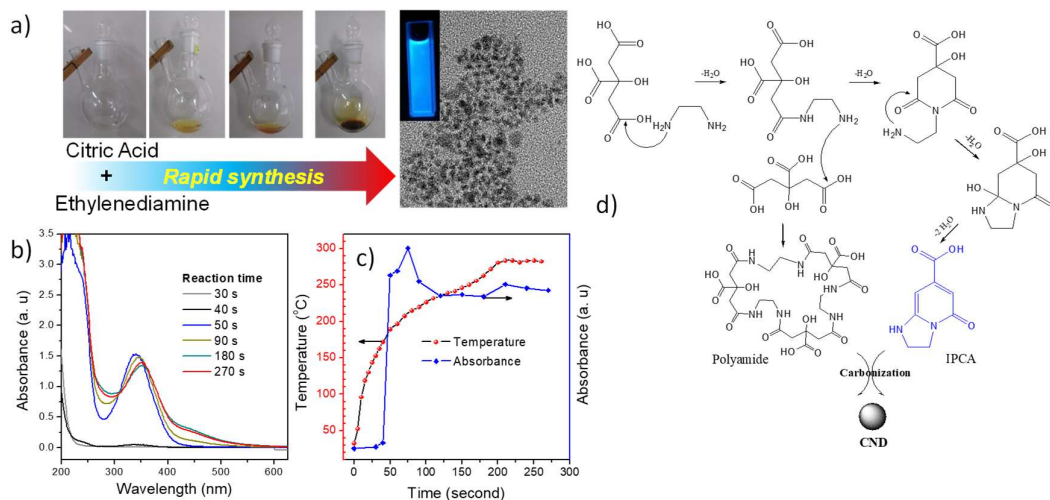


Figure 9: a) Microwave-assisted synthesis of CNDs from citric acid and ethylenediamine; b) The evolution of absorption and according to irradiated time and c) temperature [6]. d) The formation of IPCA via intramolecular condensation between citric acid and ethylenediamine [32].

B. Yang and co-workers reported the synthesis of highly photoluminescent CNDs with a quantum yield of 80% by hydrothermal treatment of citric acid (CA) and ethylenediamine (EDA) [33]. Later studies by the same group explained the absorption and emission of CNDs to be due to IPCA which is an intermediate formed via intramolecular condensation between CA and EDA, Fig. 9d [32]. In parallel, CA and EDA undergo intermolecular condensation forming polyamide that is further carbonized together with IPCA forming CNDs as theoretically modeled in Fig. 6c. IPCA can also be

formed under the ambient pressure when a solution of CA and EDA in glycerol is heated by microwave irradiation, Fig. 9a-c [6]. As the reaction temperature increases continuously IPCA starts to form at about 170°C and reaches the maximum concentration at 210°C. At higher temperature, IPCA joint carbonization process forming CNDs. IPCA fluorophore gives a distinct absorption band at 350 nm and an excitation-independent emission spectrum at 440 nm [32]. Additionally, IPCA is the main source of the broad excitation-independent photoluminescence of CNDs synthesized from CA and EDA [22].

In a similar synthetic scheme, L. Shi and co-workers used citric acid and L-cysteine or cysteamine to prepare N,S-doped CNDs and demonstrated that molecules including 5-oxo-3,5-dihydro-2H-thiazolo [3,2-a] pyridine-3,7-dicarboxylic acid (TPDCA) and 5-oxo-3,5-dihydro-2H-thiazolo [3,2-a] pyridine-7-carboxylic acid (TPCA) are the fluorophores that account for the absorption and emission properties of CNDs, Fig. 10 [34].

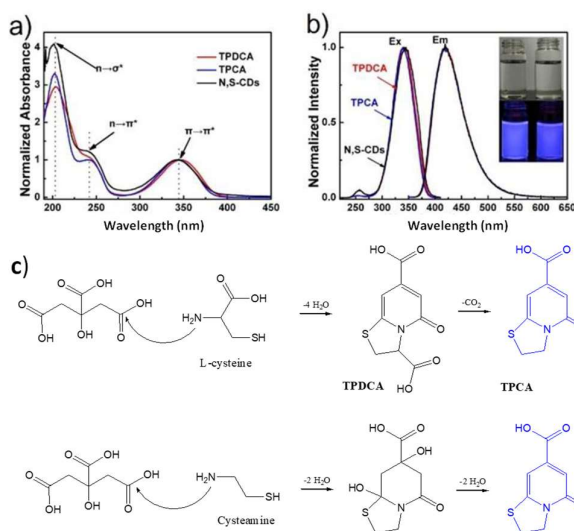


Figure 10: a) absorption; b) excitation and photoluminescent spectra of CNDs in comparison with TPDCA and TPCA. c) The formation mechanism of TPDCA and TPCA [34].

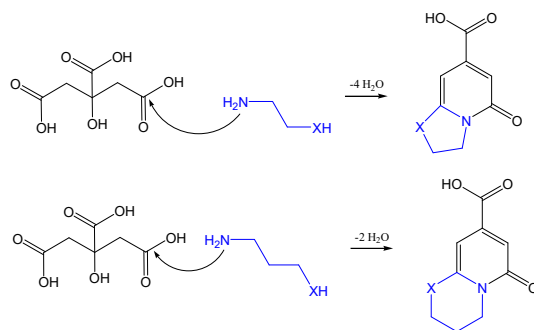


Figure 11: The formation of 5- and 6-membered ring fused 2-pyridone by the condensation between β - or γ -functional amine with citric acid [35].

By heating mixture of citric acid and diverse β - or γ - functional amines at 180°C W. Kasprzyk and co-workers found various five- or six-membered ring fused 2-pyridones, respectively, whose emission quantum yield could be high as 79% [35], Fig. 11. The scheme shown in Fig. 11 would be a good

guideline for ones to construct doped CNDs for target applications. Nevertheless, the emission color of the fluorophores is almost in the blue range where other materials such as polyamide [36], carbogenic matrix also emit.

4. Green-emitting fluorophores

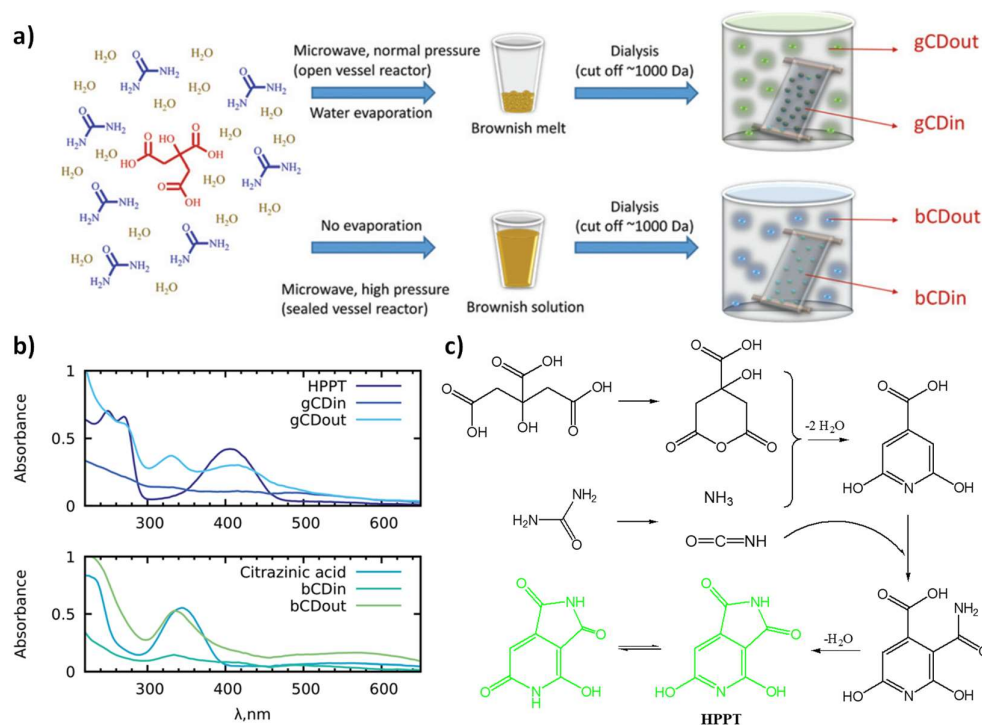


Figure 12: a) The synthesis and purification of different CNDs; b) the absorption spectra of CNDs in comparison with citrazinic acid or HPPT [37]. c) Proposed formation mechanism of HPPT [37], [38].

Urea (URA) and ethylenediamine have been used widely as N-precursor to synthesized blue-emitting CNDs. Moreover, multiple-color emitting CNDs have been prepared successfully by varying the CA/URA molar ratio and/or reaction temperature [39]. The color tuning was reasoned to a variation in surface states [40], [41], quantum confinement effects that include the graphitic domain and edge functional groups [39]. W. Kasprzyk [37] and V. Strauss [38] conducted pyrolysis CA and URA in different conditions followed by purification, Fig. 12a and chemical analysis and pointed out that citrazinic acid or 4-hydroxy-1H-pyrrolo[3,4-c]pyridine-1,3,6 (2H,5H)-trione (HPPT) fluorophores are formed respectively in closed or open reactors. CA and URA form a eutectic mixture in which CA and URA molecules bond together via hydrogen bonding. Upon heating CA is dehydrated forming anhydride while URA dissociates into ammonia and isocyanic acid. Ammonia condenses with the anhydride intermediate to form citrazinic acid that could further react with isocyanic acid forming HPPT as shown in Fig. 12c [37], [38]. HPPT accounts for a broad absorption band at 410 nm and excitation-independent emission at 540 nm of CNDs [37].

5. Red-emitting fluorophores

Using either hydrothermal or pyrolysis methods CNDs derived from citric acid (CA) usually emitting in the blue or green region. H. Lin group used formamide instead of water and could synthesized red-emitting CNDs from CA with an emission quantum yield of 22.9% [42]. The CNDs exhibit an absorption band centered at 550 nm and excitation-independent emission maximized at 640

nm. The authors claimed that the red-emission to originate from surface-related surface states [42]. K. Holá and co-workers used a solvothermal method with formamide as solvent, CA and URA as precursors to prepared CNDs which were further purified by mean of column chromatography into different color CNDs [43]. The red-emitting CNDs have an emission quantum yield of 4.0%, a broad absorption band around 550 nm and emission maxima at 640 nm. The author correlated the color shifting from blue to green, yellow, and red to increasing graphitic nitrogen in CNDs [43]. H. Ding and coauthors using a similar solvothermal method to prepared CNDs from CA and EDA and obtained red-emitting CNDs having a emission quantum yield of 53% [44]. The CNDs exhibit an absorption band around 564 nm and excitation-independent emission at 627 nm that was attributed to nitrogen-related surface states [44]. Likely, formamide solvent was the key factor resulting in red-emitting centers in CNDs. Nevertheless, the preparation of red-emitting CNDs has enhanced the deployment of CNDs in a number of biology applications [45].

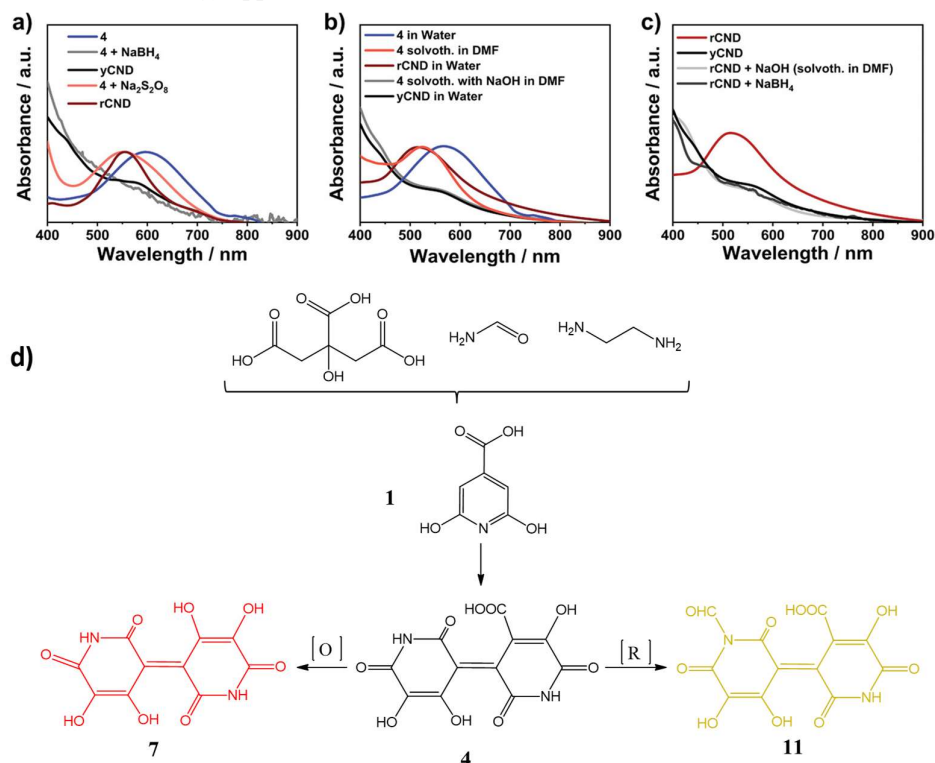


Figure 13: a) The transformations of 4 using oxidant (Na₂S₂O₈) and reductant (NaBH₄) in comparison with rCNDs and yCNDs. b) The transformations of 4 by solvothermal treatment. c) Transformations of rCNDs into yCNDs by reduction or solvothermal treatment. d) The formation mechanism of molecular fluorophores [46].

To study the molecular origin of red-emitting CNDs prepared in formamide solvent, Y. Reva and co-workers conducted solvothermal synthesis of CNDs from CA and EDA in formamide with or without NaOH and found that NaOH caused the formation of yellow-emitting CNDs (yCNDs) while red-emitting CNDs (rCNDs) were formed in the absent of NaOH [46]. By using mass spectroscopy and comparing the absorption profiles of CNDs and molecular fluorophore (denoted as 4 in Fig. 13d) the authors proposed the red- and yellow-emitting centers in yCNDs and rCNDs to originate from 4. The formation of fluorophore could be briefly presented in Fig. 13d [46]. First, CA and EDA

condensated to form citrazinic **1** which further dimerized to form **4**. **4** could be oxidized either by $\text{Na}_2\text{S}_2\text{O}_8$ (Fig. 13a) or solvothermal treatment in dimethyl formamide (DMF) (Fig. 13b) to form various fluorophores including **7** that was incorporated in rCNDs and act as red-emitting center. When **4** was reduced by NaBH_4 (Fig. 13a) or by solvothermal treatment with NaOH in DMF (Fig. 13b) it formed various forms including **11** which accounts for the yellow emission of yCNDs. The molecular origin of red-emission in rCNDs was further confirmed in Fig. 13c that show the absorption band was dismissed when rCNDs was reduced either by NaBH_4 or solvothermal treatment with NaOH in DMF.

In addition to solvothermal treatment of small organic compounds in formamide, thermal treatment of *o*-phenylenediamine (oPD) in acidic medium is another strategy that has been used recently to prepare red-emitting CNDs [47]–[51]. Despite various synthetic protocols oPD-derived CNDs exhibit very similar excitation-independent emission spectrum that involves two emitting centers around 640 nm and 680 nm. Those behaviors suggest that the emission of CNDs arises from a molecular fluorophore. Q. Zhang and coworkers proposed that 2,3-diaminophenazine (2,3-DAPN) was the main fluorophore and that the red-emission originated from protonated 2,3-DAPN [49]. Z. Peng [48] and C. K. Nandi [51] groups debated that 2,3-DAPN further polymerize forming quinoxalino[2,3-*b*]phenazine-2,3-diamine (QXPDA) fluorophore accounting for the red-emission CNDs derived from oPD. A very similar mechanism was also suggested for CNDs synthesized from oPD and catechol precursors [50]. To clarify the structure as well as the origin of the double-peak emission of oPD-derived CNDs B. Wang and coworkers prepared six different CNDs by six different methods using oPD as precursor [47]. All CNDs exhibit similar photoluminescent properties and the authors demonstrated that the emission arises from the core of CNDs and that the double-peak emission is due to electronic transition of different vibrational energy levels in the same emitting center. Based on theoretical calculations the authors suggested that the linear polymerization of 2,3-DAPN forming QXPDA was much less favorable than vertical polymerization forming graphitic structures (Fig. 14). In an earlier report, S. Yang and co-workers demonstrated experimentally that both linear and vertical polymerization of 2,3-DAPN are possible forming C_3N 2D crystals [52]. In summary, 2,3-DAPN and QXPDA are important intermediates involved in the formation of red-emitting CNDs that are synthesized using oPD.

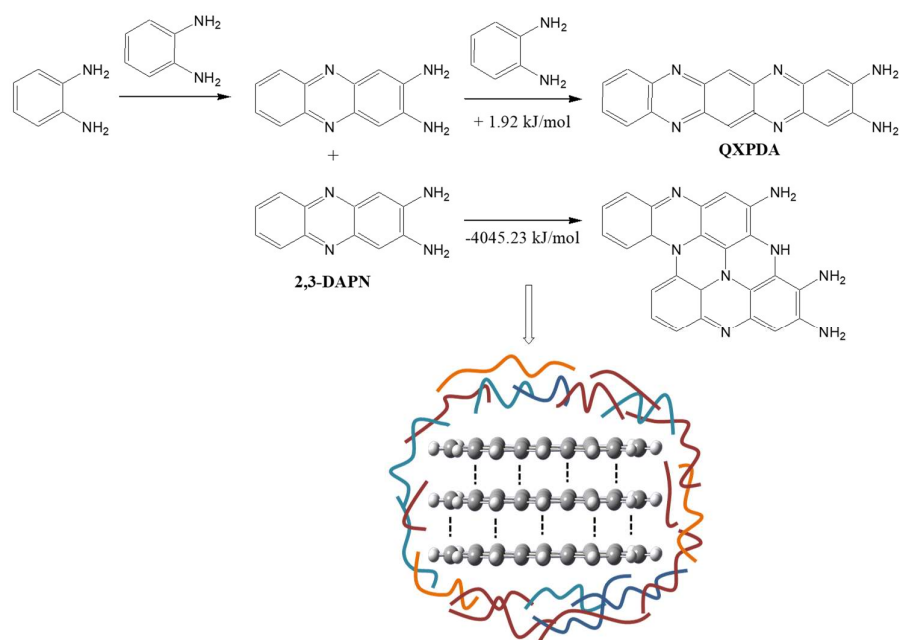


Figure 14: The formation of red-emitting CNDs from *o*-phenylenediamine [47].

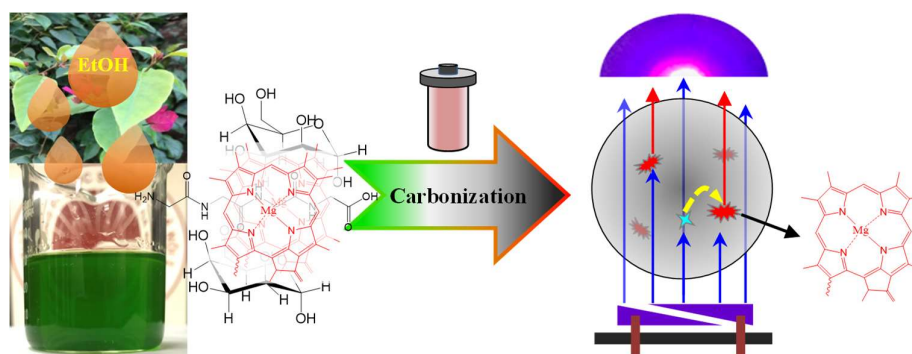


Figure 15: The preparation of red-emitting CNDs from bougainvillea leaves. Chlorophyll acts as molecular fluorophore in CNDs [53].

One of novel advantage of CNDs is that they can be synthesized from various biomass [54]. Red-emitting CNDs have been successfully synthesized using lemon and watermelon juice, bougainvillea [55], taxus and other leaves [56]. Recently, we prepared red-emitting CNDs using ethanol extract of bougainvillea and demonstrated that the red emission originates from chlorophyll fluorophore involved in carbogenic core, Fig.15 [53]. Furthermore, F. Qin and co-workers also points out that chlorophyll is the red-emitting center of leaf-derived CNDs [56]. Chlorophyll accounts for a narrow (FWHM of about 28 nm) red-emission at 670 nm and an absorption maximum at 663 nm. The bougainvillea-derived CNDs were applicable as red phosphor in horticultural LEDs [53].

6. Conclusions

Bottom-up synthesized carbon nanodots have been emerged as important building nanomaterials for diverse applications. Light absorption and photoluminescent properties are the key factors to deploy CNDs in practical uses. In this review, we have systematically summarized a class of bottom-up synthesized CNDs whose optical properties are determined dramatically by molecular fluorophores. Fluorophores are intermediate products that are formed from the carbon precursors in

the early state of thermal treatment and further being involved in carbonization polymerization processes forming CNDs. Recent reports have identified some important fluorophores such as IPCA, HPPT, and chlorophyll in blue-, green-, and red-emitting CNDs. Understandings on how fluorophores are formed and how they are involved in CNDs could help ones to adjust the synthetic protocol to obtain CNDs being suitable for a target application.

Declaration of Competing Interest

The authors declare no competing interests.

References

- [1] J. Sobhanan, J. V. Rival, A. Anas, E. Sidharth Shibu, Y. Takano, and V. Biju, "Luminescent quantum dots: Synthesis, optical properties, bioimaging and toxicity," *Adv. Drug Deliv. Rev.*, vol. 197, p. 114830, 2023, doi: 10.1016/j.addr.2023.114830.
- [2] X. Xu *et al.*, "Electrophoretic Analysis and Purification of Fluorescent Single-Walled Carbon Nanotube Fragments," *J. Am. Chem. Soc.*, vol. 126, no. 40, pp. 12736–12737, Oct. 2004, doi: 10.1021/ja040082h.
- [3] C. Y. Chung *et al.*, "Toxic or not toxic, that is the carbon quantum dot's question: A comprehensive evaluation with zebrafish embryo, eleutheroembryo, and adult models," *Polymers (Basel)*, vol. 13, no. 10, 2021, doi: 10.3390/polym13101598.
- [4] X. Yang *et al.*, "Advances, opportunities, and challenge for full-color emissive carbon dots," *Chinese Chem. Lett.*, vol. 33, no. 2, pp. 613–625, 2022, doi: 10.1016/j.ccl.2021.08.077.
- [5] D. Shen, L. Zhu, C. Wu, and S. Gu, "State-of-the-art on the preparation, modification, and application of biomass-derived carbon quantum dots," *Ind. Eng. Chem. Res.*, vol. 59, no. 51, pp. 22017–22039, 2020, doi: 10.1021/acs.iecr.0c04760.
- [6] X.-D. Mai, T. Thi Kim Chi, T.-C. Nguyen, and V.-T. Ta, "Scalable synthesis of highly photoluminescence carbon quantum dots," *Mater. Lett.*, vol. 268, p. 127595, Jun. 2020, doi: 10.1016/j.matlet.2020.127595.
- [7] V. Georgakilas, J. A. Perman, J. Tucek, and R. Zboril, "Broad Family of Carbon Nanoallotropes: Classification, Chemistry, and Applications of Fullerenes, Carbon Dots, Nanotubes, Graphene, Nanodiamonds, and Combined Superstructures," *Chem. Rev.*, vol. 115, no. 11, pp. 4744–4822, 2015, doi: 10.1021/cr500304f.
- [8] M. Fu *et al.*, "Carbon Dots: A Unique Fluorescent Cocktail of Polycyclic Aromatic Hydrocarbons," *Nano Lett.*, vol. 15, no. 9, pp. 6030–6035, 2015, doi: 10.1021/acs.nanolett.5b02215.
- [9] L. Wang *et al.*, "Full-color fluorescent carbon quantum dots," *Sci. Adv.*, vol. 6, no. 40, pp. 1–9, 2020, doi: 10.1126/sciadv.abb6772.
- [10] F. Yuan *et al.*, "Engineering triangular carbon quantum dots with unprecedented narrow bandwidth emission for multicolored LEDs," *Nat. Commun.*, vol. 9, no. 1, 2018, doi: 10.1038/s41467-018-04635-5.
- [11] H. Li *et al.*, "Water-soluble fluorescent carbon quantum dots and photocatalyst design," *Angew. Chemie - Int. Ed.*, vol. 49, no. 26, pp. 4430–4434, 2010, doi: 10.1002/anie.200906154.
- [12] F. Yuan *et al.*, "Engineering triangular carbon quantum dots with unprecedented narrow bandwidth emission for multicolored LEDs," *Nat. Commun.*, vol. 9, no. 1, p. 2249, Dec. 2018, doi: 10.1038/s41467-018-04635-5.
- [13] Y. Li, H. Shu, X. Niu, and J. Wang, "Electronic and Optical Properties of Edge-Functionalized Graphene Quantum Dots and the Underlying Mechanism," *J. Phys. Chem. C*, vol. 119, no. 44, pp. 24950–24957, 2015, doi: 10.1021/acs.jpcc.5b05935.
- [14] S. H. Jin, D. H. Kim, G. H. Jun, S. H. Hong, and S. Jeon, "Tuning the photoluminescence of graphene quantum dots through the charge transfer effect of functional groups," *ACS Nano*, vol. 7, no. 2, pp. 1239–1245, 2013, doi: 10.1021/nn304675g.
- [15] A. Sciertino, E. Marino, B. Van Dam, P. Schall, M. Cannas, and F. Messina, "Solvatochromism Unravels the Emission Mechanism of Carbon Nanodots," *J. Phys. Chem. Lett.*, vol. 7, no. 17, pp. 3419–3423, 2016, doi: 10.1021/acs.jpclett.6b01590.
- [16] R. Sato, Y. Iso, and T. Isobe, "Fluorescence Solvatochromism of Carbon Dot Dispersions Prepared from Phenylendiamine and Optimization of Red Emission," *Langmuir*, 2019, doi: 10.1021/acs.langmuir.9b02739.
- [17] M. J. Krysmann, A. Kellarakis, P. Dallas, and E. P. Giannelis, "Formation Mechanism of Carbogenic Nanoparticles with Dual Photoluminescence Emission," *J. Am. Chem. Soc.*, vol. 134, no. 2, pp. 747–750, Jan. 2012, doi: 10.1021/ja204661r.
- [18] J. Schneider *et al.*, "Molecular fluorescence in citric acid-based carbon dots," *J. Phys. Chem. C*, vol. 121, no. 3, pp. 2014–2022, 2017, doi: 10.1021/acs.jpcc.6b12519.
- [19] M. Langer *et al.*, "Progress and challenges in understanding of photoluminescence properties of carbon dots based on theoretical computations," *Appl. Mater. Today*, vol. 22, 2021, doi: 10.1016/j.apmt.2020.100924.
- [20] R. Zhao and R. Q. Zhang, "A new insight into π - π Stacking involving remarkable orbital interactions," *Phys. Chem. Chem. Phys.*, vol. 18, no. 36, pp. 25452–25457, 2016, doi: 10.1039/c6cp05485d.
- [21] Y. Song *et al.*, "Investigation from chemical structure to photoluminescent mechanism: A type of carbon dots from the pyrolysis of citric acid and an amine," *J. Mater. Chem. C*, vol. 3, no. 23, pp. 5976–5984, 2015, doi: 10.1039/c5tc00813a.
- [22] M. Langer, T. Hrivnák, M. Medved', and M. Otyepka, "Contribution of the Molecular Fluorophore IPCA to Excitation-Independent Photoluminescence of Carbon Dots," *J. Phys. Chem. C*, vol. 125, no. 22, pp. 12140–12148, 2021, doi: 10.1021/acs.jpcc.1c02243.
- [23] X. D. Mai *et al.*, "Homogeneous and highly photoluminescent composites based on in-situ formed fluorophores in PVA blends," *Mater. Lett.*, vol. 319, no. April, p. 132269, 2022, doi: 10.1016/j.matlet.2022.132269.
- [24] M. X. Dǔng *et al.*, "The thermal preparation of luminescent pmma composite using citric acid and ethylenediamine," *TNU J. Sci. Technol.*, vol. 227, no. 16, pp. 62–67, Oct. 2022, doi: 10.34238/tmu-jst.6470.
- [25] T. H. T. Dang, V. T. Mai, Q. T. Le, N. H. Duong, and X. D. Mai, "Post-decorated surface fluorophores enhance the photoluminescence of carbon quantum dots," *Chem. Phys.*, vol. 527, Nov. 2019, doi: 10.1016/j.chemphys.2019.110503.

- [26] M. Otyepka, M. Langer, M. Paloncýová, and M. Medved', "Molecular fluorophores self-organize into c-dot seeds and incorporate into c-dot structures," *J. Phys. Chem. Lett.*, vol. 11, no. 19, pp. 8252–8258, 2020, doi: 10.1021/acs.jpcllett.0c01873.
- [27] P. Duan, B. Zhi, L. Coburn, C. L. Haynes, and K. Schmidt-Rohr, "A molecular fluorophore in citric acid/ethylenediamine carbon dots identified and quantified by multinuclear solid-state nuclear magnetic resonance," *Magn. Reson. Chem.*, vol. 58, no. 11, pp. 1130–1138, 2020, doi: 10.1002/mrc.4985.
- [28] X. Mai, Y. T. H. Phan, and V. Nguyen, "Excitation-Independent Emission of Carbon Quantum Dot Solids," *Adv. Mater. Sci. Eng.*, vol. 2020, pp. 1–5, Dec. 2020, doi: 10.1155/2020/9643168.
- [29] M. Van Tuan, L. T. Phuong, V. A. Duc, N. X. Bach, and M. X. Dung, "Enhanced energy transfer in carbon quantum dot solids," *TNU J. Sci. Technol.*, vol. 225, no. 06, pp. 419–423, 2020.
- [30] C. J. Reckmeier *et al.*, "Aggregated Molecular Fluorophores in the Ammonothermal Synthesis of Carbon Dots," *Chem. Mater.*, vol. 29, no. 24, pp. 10352–10361, 2017, doi: 10.1021/acs.chemmater.7b03344.
- [31] A. Cappai, C. Melis, L. Stagi, P. C. Ricci, F. Mocchi, and C. M. Carbonaro, "Insight into the Molecular Model in Carbon Dots through Experimental and Theoretical Analysis of Citrazinic Acid in Aqueous Solution," *J. Phys. Chem. C*, vol. 125, no. 8, pp. 4836–4845, 2021, doi: 10.1021/acs.jpcc.0c10916.
- [32] Y. Song *et al.*, "Investigation from chemical structure to photoluminescent mechanism: A type of carbon dots from the pyrolysis of citric acid and an amine," *J. Mater. Chem. C*, vol. 3, no. 23, pp. 5976–5984, 2015, doi: 10.1039/c5tc00813a.
- [33] S. Zhu *et al.*, "Highly photoluminescent carbon dots for multicolor patterning, sensors, and bioimaging," *Angew. Chemie - Int. Ed.*, vol. 52, no. 14, pp. 3953–3957, 2013, doi: 10.1002/anie.201300519.
- [34] L. Shi *et al.*, "Carbon dots with high fluorescence quantum yield: The fluorescence originates from organic fluorophores," *Nanoscale*, vol. 8, no. 30, pp. 14374–14378, 2016, doi: 10.1039/c6nr00451b.
- [35] W. Kasprzyk, S. Bednarz, P. Zmudzki, M. Galica, and D. Bogdał, "Novel efficient fluorophores synthesized from citric acid," *RSC Adv.*, vol. 5, no. 44, pp. 34795–34799, 2015, doi: 10.1039/c5ra03226a.
- [36] L. Vallan *et al.*, "Supramolecular-Enhanced Charge Transfer within Entangled Polyamide Chains as the Origin of the Universal Blue Fluorescence of Polymer Carbon Dots," *J. Am. Chem. Soc.*, vol. 140, no. 40, pp. 12862–12869, 2018, doi: 10.1021/jacs.8b06051.
- [37] W. Kasprzyk, T. Świergosz, S. Bednarz, K. Walas, N. V. Bashmakova, and D. Bogdał, "Luminescence phenomena of carbon dots derived from citric acid and urea—a molecular insight," *Nanoscale*, vol. 10, no. 29, pp. 13889–13894, 2018, doi: 10.1039/c8nr03602k.
- [38] V. Strauss, H. Wang, S. Delacroix, M. Ledendecker, and P. Wessig, "Carbon nanodots revised: The thermal citric acid/urea reaction," *Chem. Sci.*, vol. 11, no. 31, pp. 8256–8266, 2020, doi: 10.1039/d0sc01605e.
- [39] X. Miao *et al.*, "Synthesis of Carbon Dots with Multiple Color Emission by Controlled Graphitization and Surface Functionalization," *Adv. Mater.*, vol. 30, no. 1, pp. 1–8, 2018, doi: 10.1002/adma.201704740.
- [40] X. Li, S. Zhang, S. A. Kulich, Y. Liu, and H. Zeng, "Engineering surface states of carbon dots to achieve controllable luminescence for solid-luminescent composites and sensitive Be²⁺ detection," *Sci. Rep.*, vol. 4, pp. 1–8, 2014, doi: 10.1038/srep04976.
- [41] T. Hu *et al.*, "Temperature-controlled spectral tuning of full-color carbon dots and their strongly fluorescent solid-state polymer composites for light-emitting diodes," *Nanoscale Adv.*, vol. 1, no. 4, pp. 1413–1420, 2019, doi: 10.1039/c8na00329g.
- [42] S. Sun, L. Zhang, K. Jiang, A. Wu, and H. Lin, "Toward High-Efficient Red Emissive Carbon Dots: Facile Preparation, Unique Properties, and Applications as Multifunctional Theranostic Agents," *Chem. Mater.*, vol. 28, no. 23, pp. 8659–8668, 2016, doi: 10.1021/acs.chemmater.6b03695.
- [43] K. Holá *et al.*, "Graphitic Nitrogen Triggers Red Fluorescence in Carbon Dots," *ACS Nano*, vol. 11, no. 12, pp. 12402–12410, 2017, doi: 10.1021/acsnano.7b06399.
- [44] H. Ding, J. S. Wei, N. Zhong, Q. Y. Gao, and H. M. Xiong, "Highly Efficient Red-Emitting Carbon Dots with Gram-Scale Yield for Bioimaging," *Langmuir*, vol. 33, no. 44, pp. 12635–12642, 2017, doi: 10.1021/acs.langmuir.7b02385.
- [45] A. Lv *et al.*, "Long-wavelength (red to near-infrared) emissive carbon dots: Key factors for synthesis, fluorescence mechanism, and applications in biosensing and cancer theranostics," *Chinese Chem. Lett.*, vol. 32, no. 12, pp. 3653–3664, 2021, doi: 10.1016/j.ccllet.2021.06.020.
- [46] Y. Reva *et al.*, "Understanding the Visible Absorption of Electron Accepting and Donating CNDs," *Small*, vol. 2207238, pp. 1–10, 2023, doi: 10.1002/smll.202207238.
- [47] B. Wang *et al.*, "Electron–phonon coupling-assisted universal red luminescence of o-phenylenediamine-based carbon dots," *Light Sci. Appl.*, vol. 11, no. 1, 2022, doi: 10.1038/s41377-022-00865-x.
- [48] C. Ji *et al.*, "Phenylenediamine-derived near infrared carbon dots: The kilogram-scale preparation, formation process, photoluminescence tuning mechanism and application as red phosphors," *Carbon N. Y.*, vol. 192, pp. 198–208, Jun. 2022, doi: 10.1016/j.carbon.2022.02.054.
- [49] Q. Zhang, R. Wang, B. Feng, X. Zhong, and K. (Ken) Ostrikov, "Photoluminescence mechanism of carbon dots: triggering high-color-purity red fluorescence emission through edge amino protonation," *Nat. Commun.*, vol. 12, no. 1, pp. 1–13, 2021, doi: 10.1038/s41467-021-27071-4.
- [50] P. Li *et al.*, "Formation and fluorescent mechanism of red emissive carbon dots from o-phenylenediamine and catechol system," *Light Sci. Appl.*, vol. 11, no. 1, pp. 1–11, 2022, doi: 10.1038/s41377-022-00984-5.
- [51] N. Soni *et al.*, "Absorption and emission of light in red emissive carbon nanodots," *Chem. Sci.*, vol. 12, no. 10, pp. 3615–3626, 2021, doi: 10.1039/d0sc05879c.
- [52] S. Yang *et al.*, "C₃N—A 2D Crystalline, Hole-Free, Tunable-Narrow-Bandgap Semiconductor with Ferromagnetic Properties," *Adv. Mater.*, vol. 29, no. 16, pp. 1–7, 2017, doi: 10.1002/adma.201605625.
- [53] X.-D. Mai, S.-H. Nguyen, D.-L. Tran, V.-Q. Nguyen, and V.-H. Nguyen, "Single-chip horticultural LEDs enabled by greenly

- synthesized red-emitting carbon quantum dots,” *Mater. Lett.*, vol. 341, no. March, p. 134195, 2023, doi: 10.1016/j.matlet.2023.134195.
- [54] W. Meng, X. Bai, B. Wang, Z. Liu, S. Lu, and B. Yang, “Biomass-Derived Carbon Dots and Their Applications,” *Energy Environ. Mater.*, vol. 2, no. 3, pp. 172–192, 2019, doi: 10.1002/eem2.12038.
- [55] P. Khare, A. Bhati, S. R. Anand, Gunture, and S. K. Sonkar, “Brightly Fluorescent Zinc-Doped Red-Emitting Carbon Dots for the Sunlight-Induced Photoreduction of Cr(VI) to Cr(III),” *ACS Omega*, vol. 3, no. 5, pp. 5187–5194, 2018, doi: 10.1021/acsomega.8b00047.
- [56] F. Qin *et al.*, “Searching for the true origin of the red fluorescence of leaf-derived carbon dots,” *Phys. Chem. Chem. Phys.*, vol. 25, no. 4, pp. 2762–2769, 2023, doi: 10.1039/D2CP05130C.